LIMNOLOGY and OCEANOGRAPHY

ASLO

Limnol. Oceanogr. 68, 2023, 1001–1018

doi: 10.1002/lno.12319

Under-ice plankton community response to snow removal experiment in bog lake

Ellie Socha,* **Adrianna Gorsky**, **Noah R. Lottig**, **Gretchen Gerrish**, **Emily C. Whitaker**, **Hilary A. Dugan**

Center for Limnology, University of Wisconsin-Madison, Madison, Wisconsin, USA

Abstract

Although previously overlooked, winter is now seen as a period of significant biological activity in the annual cycle of north-temperate lakes. Research suggests a future of reduced ice cover duration and altered snow conditions could significantly change the functioning of aquatic ecosystems. This study seeks to explore the possible repercussions of changing ice and snow dynamics on aquatic biological communities, particularly at lower trophic levels. To explore plankton community responses to changing under-ice light conditions, we performed a whole-lake manipulation by removing all of the snow from the surface of a north temperate bog lake in northern Wisconsin. Over three winters, samples were collected under ice in the study lake, South Sparkling Bog. The first winter, 2018–2019, served as a reference year during which snow was not removed from the lake and was followed by two subsequent winters of snow removal during 2019–2020 and 2020–2021. Data collected included phytoplankton and zooplankton abundances and taxa, chlorophyll *a*, dissolved organic carbon, light, Secchi depth, and ice and snow thickness. In our snow removal years, increased light availability in the water column shifted the phytoplankton community from low-biomass, mixed community of potential mixotrophs, unicellular cyanobacteria and Chlorophytes to dominance by photoautotrophs, and rotifer zooplankton densities increased. Ice condition, specifically the thickness of white ice vs. black ice, was a major driver in the magnitude of change between years. This research improves our understanding of how plankton communities might respond to climate-change driven shifts in winter dynamics for north temperate systems.

Roughly half of the lakes on Earth experience some annual ice cover, and over the last century, many of these lakes have experienced a decline in the duration of lake ice cover (Sharma et al. 2021; Imrit and Sharma 2021). As lake ice duration shortens, it is projected that average lake ice thickness could decline by ~0.35 m for 1300 of the world's largest lakes in coming years (Li et al. 2021) due to rapidly warming winter air temperatures (Shatwell et al. 2019). It is also predicted that as winters warm, the relative thickness of white ice to black ice will increase (Weyhenmeyer et al. 2022). Concomitant with warming winters are projected changes in winter snowpack. In North America, long-term observations reveal changes in snowpack (increases in early winter, decreases in late winter/spring), earlier maximum mountain snow-water-equivalent, and earlier springtime snow melt (Lemke et al. 2007). Earlier springtime snow melt has decreased average snow cover duration by 5.3 d per decade from 1972 to 2008 in the Northern Hemisphere (Choi et al. 2010).

If the snow cover and ice conditions on lakes change, there will be feedbacks on lake physics, biogeochemical cycling, and biology (Cavaliere et al. 2021). Snow cover influences food webs through the insular properties of snow; reflectance of solar radiation and reduction of light transmission, which reduces the availability of photosynthetically active radiation (PAR); and timing of phenological events, especially with earlier onset of snow melt and springtime conditions (Penczykowski et al. 2017; Hrycik et al. 2021; Slatyer et al. 2022). The limited availability of PAR in ice-covered lakes constrains primary productivity (Katz et al. 2015), likely much more so than temperature or nutrient limitation. It is this light constraint that led early seasonal models of

*Correspondence: elliesocha@gmail.com

Additional Supporting Information may be found in the online version of this article.

Author Contribution Statement: E.S., A.G., and E.W. coordinated field sampling, and E.S. performed all zooplankton analyses with support from G.G. N.L. and H.D. designed the experiment and oversaw all operations, including data management. E.S. and H.D. led the development of this manuscript.

phytoplankton ecology to dismiss winter as a time of reduced primary production (Sommer et al. 1986). However, despite light limitation, phytoplankton can be abundant under ice! There have been many recorded observations of phytoplankton blooms occurring under lake ice (Vanderploeg et al. 1992; Phillips and Fawley 2002; Yang et al. 2020), even in extremely light limited environments (Tanabe et al. 2007). Furthermore, some phytoplankton species use mixotrophy for heterotrophic carbon acquisition, which circumvents light limitation (Marshall and Laybourn-Parry 2002; Patriarche et al. 2021).

In the few winter lake studies that detail under-ice phytoplankton communities, flagellates, dinoflagellates, diatoms, and cyanobacteria are most common (Phillips and Fawley 2002; Blank et al. 2009; Lenard and Ejankowski 2017; Öterler 2017). These groups are typically well adapted to survive winter conditions. However, as lakes experience a decrease in lake ice duration and snow cover, phytoplankton communities (in north temperate climates) are expected to shift in dominance toward taxa that are more suited to water column mixing and have higher light requirements, and away from species that are motile and mixotrophic (Özkundakci et al. 2016; Hampton et al. 2017). Declining ice cover has the potential to alter entire planktonic food webs by impacting the timing, magnitude, and presence of winter phytoplankton blooms. Therefore, changing ice conditions portends food web regime shifts and displaced plankton phenology (Wollrab et al. 2021).

The role of light availability in the water column is consequential to under-ice productivity, and likely has feedbacks on trophic interactions. Hrycik and Stockwell (2021) showed the importance of light limitation in structuring phytoplankton community characteristics in a shallow hypereutrophic lake, and found that zooplankton grazing significantly reduced diatoms and cryptophyte biomass. Freshwater zooplankton employ a variety of strategies to successfully overwinter. In general, most groups use diapause, or dormancy, as a mechanism to avoid unfavorable environmental conditions. The induction and termination of dormancy varies across groups, but it is often related to physical conditions, namely, temperature and photoperiod (de Senerpont Domis et al. 2007). However, dormancy is not the only path to winter survival. Cladocerans, such as *Daphnia*, are known to produce diapause eggs, or ephippium, in addition to overwintering by lowering their physiological rates. Certain cladocerans are also able to reproduce under ice (Allan 1977), and some copepod species are known to remain relatively active during the winter (Grosbois and Rautio 2018). In addition, rotifers can proliferate and account for the majority of abundance and biomass of winter zooplankton communities (Virro et al. 2009; Kalinowska and Grabowska 2016). Despite the possible array of overwintering strategies among all groups, the driving factors in shaping under-ice zooplankton communities are not well understood.

Here, we report on a whole-lake manipulation aimed at investigating the importance of light in structuring under-ice ecosystem characteristics and plankton dynamics. We hypothesized that light is the primary driver of under-ice biological processes, and that snow and ice characteristics impact the under-ice light environment. To test this hypothesis, we experimentally removed winter snow accumulation from the top of a bog lake for the entirety of two winters (2019–2020 and 2020–2021). By doing so, we aimed to reduce the amount of snow and opaque white ice and increase the proportion of transparent black ice that lets more light penetrate into the water column. The 2018–2019 winter season served as a reference year. We predicted that snow clearing and the subsequent increased light availability would support more primary production by phototrophic phytoplankton, and result in greater phytoplankton biovolume. We expected that increases in phytoplankton biovolume would act as a larger available energy source for grazers, and thus, would support greater densities of consumers (zooplankton).

Methods

Study site

South Sparkling Bog (46.003°N, 89.705°W), is a dystrophic, dimictic bog lake with a maximum depth of 8 m, a mean depth of 3.6 m, and a surface area of 0.44 ha, located in Vilas County in Northern Wisconsin (Fig. 1). South Sparkling Bog is surrounded by a sphagnum bog mat, has no shoreline development, and is characterized by high concentrations of dissolved organic carbon (DOC) and nutrients: pH 4.5–4.9, DOC 16.8–27.2 mg L^{-1}, total dissolved phosphorus 16.3–18.2 μg L^{-1}, and total dissolved nitrogen 451.6–1179.2 μg L^{-1}. Secchi depths are routinely < 1 m.

Snow manipulation

During the winters of 2019–2020 and 2020–2021, snow was removed from the surface of South Sparkling Bog. Removal was conducted via a snowblower and a snowplow attached to the front of an ARGO all-terrain vehicle. The winter of 2018–2019 served as a reference year with no snow removal.

Sample and data collection

An under-ice buoy was deployed to collect measurements every 10 min of temperature (°C), dissolved oxygen (% and mg L^{-1}, PME MiniDot), and light intensity (Lumen m^{-2}, Onset HOBO Pendant). The dissolved oxygen sensor was at 0.7 m, a depth that would prevent it from freezing into the ice. Light loggers were located at 0.70, 1.20, 1.45, 1.95, 2.95, 4.45, and 7.45 m depth. The buoy was deployed away from any sampling holes to prevent any alteration to the ice and snow conditions above the buoy. Because of this, the buoy was not maintained during the winter. Biofouling of the sensors was present in the spring, but given the rapid response of both oxygen and light readings to ice and snow conditions, we believe that biofouling did not significantly affect data collection.

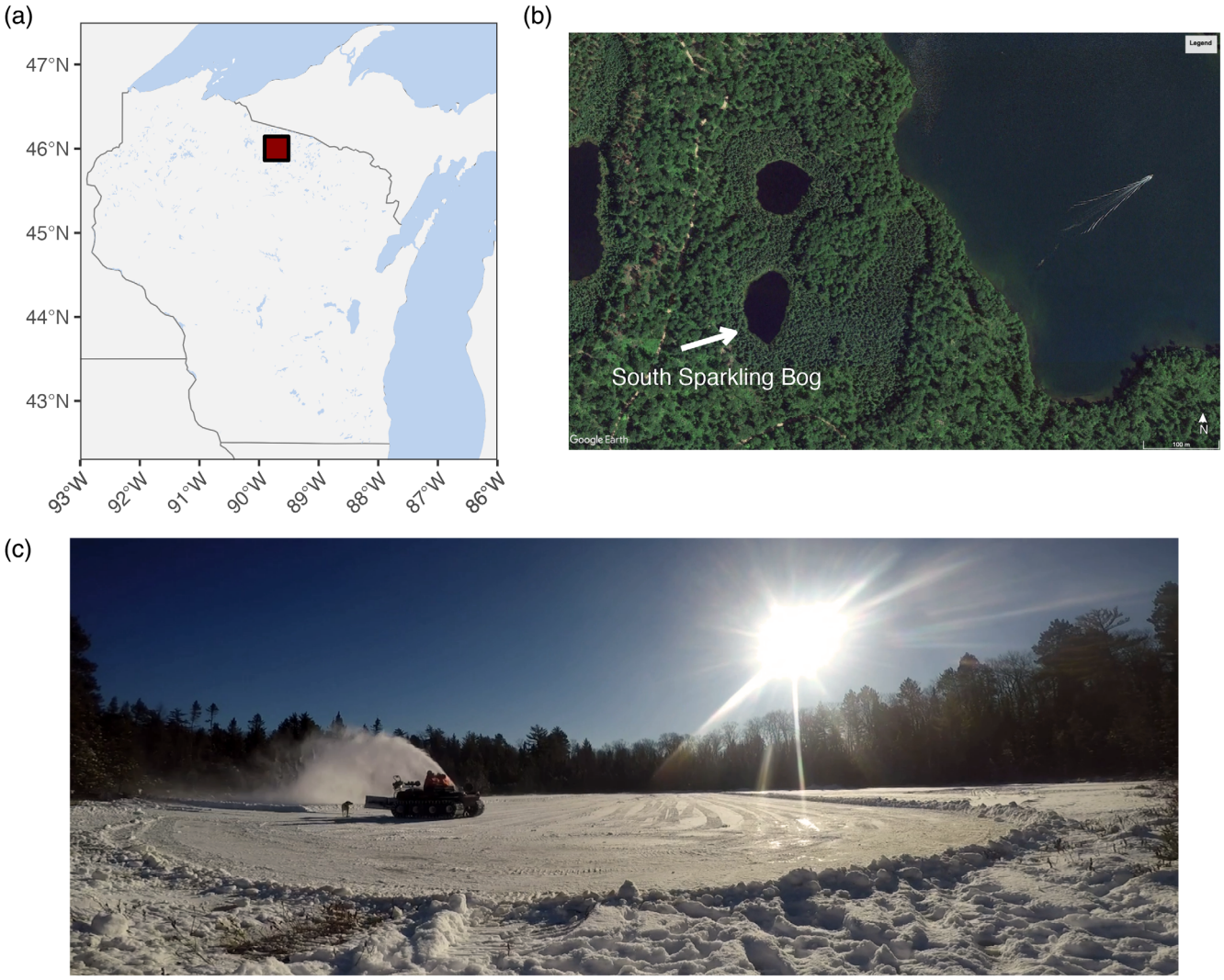

Fig. 1. (**a**) Site map showing the location of South Sparkling Bog in Northern Wisconsin, and (**b**) a satellite image showing the forested watershed surrounding the bog. Source: Google Earth imagery. (**c**) The bog being actively plowed in 2021.

South Sparkling Bog was manually sampled monthly to biweekly throughout the winters (January through mid-April) of 2019, 2020, and 2021 (Supporting Information Table S1). All samples were collected in the middle of the lake where the maximum depth was 8 m. Samples were taken from an ice hole drilled with an 8-in. diameter gas auger. The 0 m sampling depth is relative to the bottom of the ice cover. Manual measurements for temperature (°C), dissolved oxygen (mg L^{-1} and %), pH, and electrical conductivity ($\mu S\ cm^{-1}$) were collected at each meter (until a depth of 7 m) using a YSI Pro ODO meter. Secchi depth (m) measurements were made through the ice hole as a proxy for light attenuation solely from the water column (i.e., unrelated to ice/snow attenuation). Other physical data obtained included snow depth (cm), and black and white ice thickness (cm). Snow depth was determined by averaging 10 random samples taken with a meter stick. Total ice, black ice, and white ice thicknesses were measured in the auger hole.

Underwater PAR data were collected at 0.25 m increments using a LiCor 192 quantum sensor on an "L"-shaped boom, where the sensor was lowered through the ice hole, and then cantilevered out 1.5 m under the ice to avoid capturing light from the ice hole. A LI1400 logger was used to record underwater PAR readings as well as surface PAR using a LI190 sensor. On most sampling days in 2019, a combination of low surface PAR, and very low underwater PAR, resulted in no measurable signal. In 2020, the LI1400 logger program failed. Therefore, only PAR data from 2021 are used in this manuscript. Light attenuation coefficients for the water column in 2021 ($K_{d\ lake}$) were calculated as the negative slope of the linear regression of $\ln(light_z/light_{surface}) \sim z$, where light is measured in $\mu mol\ m^{-2}\ s^{-1}$, and depth (z) is in meters. For the

4 sampling days with surface light > 200 μmol m^{-2} s^{-1}, light transmittance through the ice was calculated by dividing the light measurements directly below the ice cover with the surface reading. A single light attenuation coefficient for ice on South Sparkling Bog ($K_{d\ ice}$) was calculated by minimizing the loss function of $\sum\left((\exp(-K_{dice} \times \text{Ice Thickness}) - \text{Light Transmission})^2\right)$ on the 4 sampling days, where ice thickness is measured in meters, and light transmission as a fraction (similar to Arndt et al. 2017). Using manual PAR measurements from 2021, we constructed a linear model to relate light intensity readings from the buoy to PAR using ordinary least squares regression. The resulting equation was $\text{PAR} = 10^{0.9094 \times \log_{10}(\text{lux}) - 1.9934}$ ($r^2 = 0.876$), where lux is light intensity in lum m^{-2}.

Phytoplankton samples were obtained from 0 to 3 m and 3 to 7 m by slowly lowering weighted Tygon tubing through the water column to a depth of 7 m, such that the tubing was filled with a representative water column sample. Based on the inner diameter of the tubing, 205 mL of water was pumped from the tubing for the upper sample. Next, 267 mL of water was pumped from the tubing for the lower sample. Each sample was collected into a 250-mL amber bottle that contained 2 mL of Lugol's solution. Phytoplankton samples were pooled by sampling date and sent to Phycotech Inc. for phytoplankton identification, and concentration and biovolume quantification. Chlorophyll *a* (Chl *a*) samples were obtained at depths of 0, 2, 3, 5, and 7 m with an additional random duplicate depth for quality control. At each depth, water was pumped through Tygon tubing attached to a peristaltic pump and filtered through in-line filter cartridges holding a 47-mm-type A/E glass fiber filter. At each depth, water was pumped and filtered until 500 mL was collected or 15 psi was measured via an attached pressure gauge. Filters were stored away from light and frozen prior to laboratory analysis. Chlorophyll samples were analyzed via fluorometry using the North Temperate Lakes US Long-Term Ecological Research Network (NTL-LTER) protocols to determine concentrations in μg L^{-1} (NTL-LTER 2022).

Integrated zooplankton tows were taken from 0 to 7 m depth using a 56-μm mesh Wisconsin net. All zooplankton samples were collected into glass sample jars, preserved in 90% ethanol, and saved for laboratory analysis. In the lab, zooplankton samples were filtered through 53-μm mesh and diluted to a known volume, and three subsample replicates were taken using a 1-mL Hensen-Stempel pipette. Subsample replicates were counted to at least 100 individuals, otherwise the entire sample was quantified. Subsample data were then converted to the known diluted volume and finally converted to total filtered volume (from the integrated tow sample) to estimate density (individuals L^{-1}). Zooplankton samples were visualized and quantified using a Leica M8Z dissecting scope and Leica imaging software. Replicate subsamples were averaged to estimate total abundance and density, and average lengths (mm) for each sample taxa were calculated from measures of the first 30 individuals of each taxon found within a sample date. Additional imaging for morphological observation was obtained using a Nikon ECLIPSE Ci series compound microscope and NIS-Elements D 5.20.00 software at ×200 and ×400 magnifications.

Water samples for analysis of dissolved reactive silica and dissolved and total inorganic and organic carbon (DRSi, DIC, TIC, DOC, TOC) were taken at depths of 0, 3, and 7 m with an additional random duplicate depth for quality control. All sample collection jars were rinsed three times prior to collection. Samples for dissolved carbon were filtered through a 0.40-μm polycarbonate in-line filter, and all carbon samples were kept in a dark area and refrigerated until analysis. Watery quality samples were analyzed by the NTL-LTER Water Chemistry Lab and followed NTL-LTER protocols (NTL-LTER 2020).

Data analysis

Phytoplankton were analyzed by their taxonomic division, as well as grouped by morphofunctional classifications (Salmaso and Padisák 2007). There were five morphofunctional groups in the phytoplankton community: (1) large (unicellular or colonial) potential mixotrophs, (2) small (unicellular) potential mixotrophs, (3) unicellular cyanobacteria, (4) colonial cyanobacteria, and (5) other large, unicellular, nonflagellates (mostly Chlorophytes). We summarized relative total biovolume and biovolume (μg L^{-1}) by division and morphofunctional groupings. Zooplankton data were used to calculated density (individuals L^{-1}), relative taxa abundance, biomass (μg L^{-1}), and species richness. Zooplankton were summarized by genera as well as trophi structure functional groupings based on Oh et al. (2017). Trophi structure is a taxonomic characteristic that describes the morphology of a rotifer's feeding apparatus and provides insight into feeding behavior. There were five trophi structure functional groupings present in the zooplankton community: (1) Virgate trophi 1, (2) Virgate trophi 2, (3) Incudate trophi, (4) Malleate trophi, and (5) "N/A" or other (when rotifer taxonomic classification was not possible, or taxa did not possess trophi parts). These trophi groupings can be further classified by feeding strategy (Obertegger et al. 2011). Virgate trophi groups and the incudate trophi group are generally known as "raptorial" feeders. This denotes that they consume single food particles by "grasping, piercing, or pumping" movements that are independent of their trophi and body size. The malleate trophi group is considered "microphagous" meaning they are limited by trophi size and ingest multiple small food items (less than 20 μm) at once.

To visualize multiple dimensions and relate potential environmental drivers to phytoplankton and zooplankton community composition, we performed two constrained ordination techniques: redundancy analysis (RDA) and canonical correspondence analysis (CCA). RDA is a linear method, and proved more effective for exploring the effect of environmental drivers on phytoplankton. Explanatory variables in the final model were $\log_{10}$(PAR at 0.7 m) + black ice thickness + white ice thickness + Secchi depth. Snow and total ice thickness were not included, as they co-varied with other drivers. PAR was extracted as the daily mean from the buoy

sensors. Our goal was to create the most parsimonious model where the final model was chosen based on significance, relevance to our hypotheses, and minimizing total variables and variable correlation. We tested two groupings of phytoplankton community data: (1) $\log_{10}$ abundance of Cyanophyta, Chlorphyta, and Chrystophta, plus $\log_{10}$ total phytoplankton biovolume and (2) log abundance phytoplankton grouped by morphofunctional group (Salmaso and Padisák 2007).

For zooplankton, CCA models (unimodal models) resulted in better explanatory relationships between zooplankton community data and environmental variables. Explanatory variables were based on the biological inference that phytoplankton communities should influence zooplankton densities. Variables included $\log_{10}$ total phytoplankton biovolume as well as $\log_{10}$ total biovolume of Chlorophyta and Cyanophyta, as these were the two dominant groups. Mean daily PAR was also included as it was the most significant driver from the phytoplankton RDA. We tested two groupings of zooplankton community data: (1) total density of zooplankton grouped by genera present on three or more sampling days; and (2) total density of zooplankton grouped by trophi structure groups (Oh et al. 2017). ANOVA like permutation tests for the joint effect of constraints in the RDAs and CCAs were used to test the significance of the full models, individual terms, and the first two axes. The terms are assessed sequentially, and the order of the terms will influence their significance. Since these are permutation tests, the absolute value of the *p*-values will change slightly on every run.

To statistically analyze differences between phytoplankton and zooplankton community composition, we used analysis of similarities (ANOSIM) tests, where a dissimilarity matrix was calculated using the Bray method. We also computed Shannon diversity (H') for both phytoplankton (species level where possible) and zooplankton (genus level) communities for each sample date using the equation:

$$H' = -\sum_{i=1}^{s} p_i \ln(p_i)$$

where H' = Shannon diversity index, p_i = proportion of individuals of i^{th} species in the community, and s = the total number of species in the community. Statistical analyses and visualizations were conducted using R version 4.2.1 (R Core Team, 2021), with tidyverse (Wickham et al. 2019), lubridate (Grolemund and Wickham 2011), patchwork (Pedersen 2022), vegan (Oksanen et al. 2020), corrr (Kuhn et al. 2020), and ggrepel (Slowikowski 2021).

Results

Physical conditions (Year 1: Snow, Year 2: White ice, Year 3: Black ice)

South Sparkling Bog winter climate conditions were similar during the 3 years of study, which is reflected in the dates of ice-onset and breakup and the overall duration of lake ice. Ice duration during reference and snow-removal years was 155, 169, and 140 d, respectively, and all years received > 1 m of snowfall (Supporting Information Table S2). Our success in altering the snow and ice characteristics on South Sparkling Bog via snow removal is evident from the comparison of the ice conditions in the manipulation years to the reference year. Across the 3 years, white ice thickness ranged from 11.5 to 48 cm (Year 1), 2 to 24 cm (Year 2), and 0 to 10.5 cm (Year 3). Removing snow on South Sparkling Bog resulted in a greater proportion of black ice to white ice compared to the reference year (Fig. 2a), as white ice primarily forms for overlying snow (Ariano and Brown 2019).

The greater white ice proportion in Year 2 is attributed to the timing of initial ice formation and local weather conditions. During freeze-up on 06 November 2019 and shortly thereafter, the surrounding area received considerable and consistent snowfall. During this time, South Sparkling Bog's ice conditions were not safe enough for sampling or snow removal, and it was effectively impossible to prevent the subsequent early formation of white ice. These conditions then persisted for the remainder of the winter. The freeze-up weather conditions were very different in Year 3, when ice-on occurred on 16 November 2020, and the surrounding area received little-to-no measurable snowfall until mid-December. Under these conditions, the early ice cover on South Sparkling Bog (and all lakes in the area) was entirely black ice, and by the time snow removal was necessary, the black ice was thick enough to safely support the field crew. The outcome of our manipulation compounded with early winter climate, resulted in three distinct years of investigation, which we refer to as: Year 1: snow, Year 2: white ice, and Year 3: black ice.

Mean daily under-ice PAR was < 1 μmol m^{-2} s^{-1} on all sampling days in Years 1 and 2, but ranged from 0.8 to 11 μmol m^{-2} s^{-1} in Year 3 (Fig. 2b). From the under-ice buoy, PAR peaked at a mean daily PAR of 16.2 μmol m^{-2} s^{-1} and maximum daily PAR of 80.2 μmol m^{-2} s^{-1} in the weeks preceding ice-off in Year 3 (Fig. 3b). That year, transmission of light through the ice ranged from 12% to 32%, and across the year, the ice had a calculated K_d of 4.45 (Table 1). In Years 2 and 3, increases in PAR coincided with increases in dissolved oxygen just prior to ice off. The only time dissolved oxygen was measurable (0–1% saturation) was during periods of increased PAR (Fig. 3c). PAR at 0.7 m was negatively correlated to white ice and snow thickness (Fig. 4).

Secchi depth also decreased in Years 2 and 3. In Year 1, Secchi depths were 70–90 cm, compared to 32–62 cm in the two snow removal years (Fig. 2c). Calculated K_d of the water column in Year 3 ranged from 1.65 to 4.24 (Table 1). Linear correlation of environmental variables shows a positive correlation between snow thickness, white ice thickness, and Secchi depth, and a negative correlation with black ice thickness and Chl *a* concentration (Fig. 4). Due to some missing

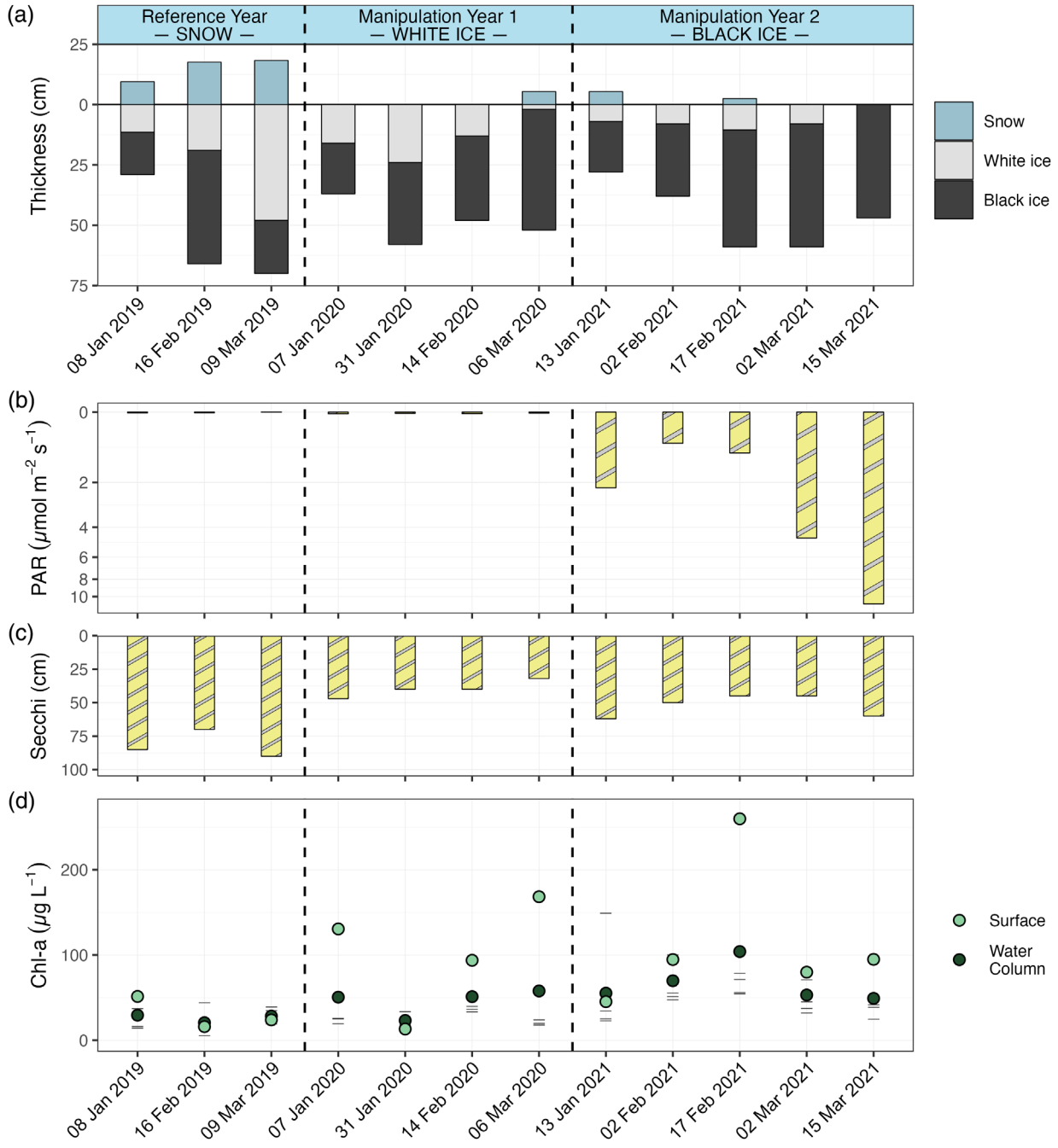

Fig. 2. (**a**) South Sparkling Bog snow and ice thickness by sampling date in the three study years. Zero on the *y*-axis represents the lake surface, with snow thicknesses above zero, and ice thickness below zero. (**b**) Mean underwater PAR on the sampling day. PAR was modeled from the top light intensity sensor (0.7 m) on the submerged buoy (**c**) Secchi depth measurements. (**d**) Chl *a* concentrations (μg L^{-1}) for each winter sampling event at 0, 2, 3, 5, and 7 m (horizontal dashes), highlighting surface (0 m, light green), and mean (dark green) concentrations.

and flagged DOC and TOC results, it was not possible to statistically compare concentrations between years. However, the data that passed quality control did not indicate any changes in DOC between years. DOC concentrations in the top 0–3 m over the 3 yr ranged from 19.3 to 19.7, 16.8 to 22.0, and 16.8 to 21.8 mg L^{-1}, respectively (Supporting Information Table S3).

Phytoplankton

Chl *a* concentrations were greater in snow removal years, with a maximum observed surface concentration of 260 μg L^{-1} on 17 February 2021 (Fig. 2). In Years 2 and 3, surface Chl *a* increased up to 500%, and mean Chl *a* concentrations in the water column were consistently at least twice as high as Year 1 concentrations. Surface Chl

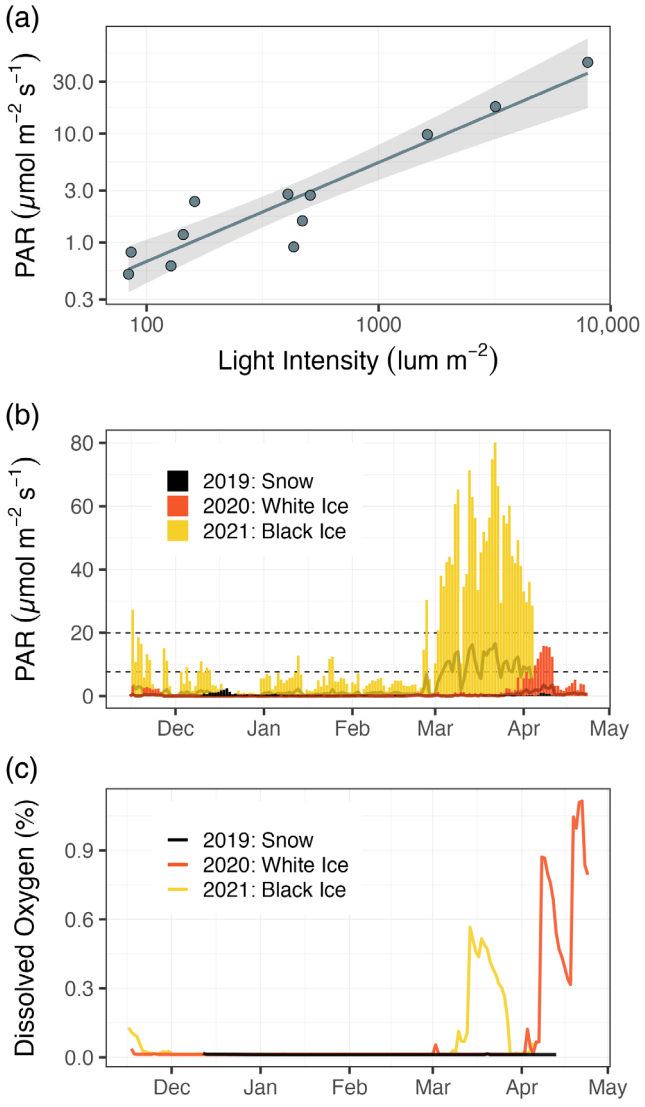

Fig. 3. (**a**) Light intensity buoy readings vs. manual PAR measurements in 2021. Sensor depths were within 0.25 m of each other. (b) Daily maximum (bars), and mean (lines) PAR (μmol m^{-2} s^{-1}) as recorded by the moored buoy in South Sparkling Bog at 0.7 m depth. Dashed lines denote 7.6 and 20 μmol m^{-2} s^{-1}, which are literature thresholds for photosynthesis and biomass accumulation (Gosselin et al. 1985). (**c**) Daily maximum dissolved oxygen saturation at 0.7 m depth.

a concentrations were negatively correlated to snow, white ice thickness, and Secchi depth (Fig. 4).

We observed eight different taxonomic divisions of phytoplankton in winter samples from South Sparkling Bog (Fig. 5; Supporting Information Table S4). Shannon diversity values ranged from 0.27 to 1.47 and were greatest during Year 3 (Supporting Information Fig. S1). Phytoplankton total biovolume increased each year of the study (2019: mean = 0.897×10^{-6} μm^3 mL^{-1}; 2020: mean = 1.77×10^{-6} μm^3 mL^{-1}; 2021: mean = 6.58×10^{-6} μm^3 mL^{-1}; Fig. 5). During Year 1, Chlorophyta dominated the phytoplankton community and comprised 43.8% of relative total biovolume; Cyanophyta and Chrysophyta contributed 32.3% and 19.2% to total biovolume, respectively. Snow removal years had sizeable shifts in the divisional composition of total phytoplankton biovolume, and Chlorophyta increased in dominance. Relative total biovolume of Chlorophyta increased from 43.8% in Year 1 to 84.0% in Year 2 and 68.0% in Year 3 (Fig. 5b; Supporting Information Table S5).

Morphofunctional groupings revealed the presence of five distinct groups: small potential mixotrophs, large potential mixotrophs, unicellular cyanobacteria, colonial cyanobacteria, and other large, nonflagellated, unicellular phytoplankton (Supporting Information Table S6). With the exception of two sampling dates, large, nonflagellated, unicellular phytoplankton (primarily Chlorophytes) dominated community biovolume in each year (Fig. 5d). Combined, small and large potential mixotrophs had their greatest relative total biovolume at 31.2% during Year 1 (Fig. 5c; Supporting Information Table S6).

Grouping both by division and morpho-functional group, ANOSIM tests revealed significant ($p < 0.05$) differences between phytoplankton community biovolume between years (Table 2). Significant differences in relative biovolume were only present when phytoplankton were grouped by morphofunctional group.

Zooplankton

A total of 11 genera and 12 species of zooplankton were identified from the 3 yr of South Sparkling Bog under-ice samples (Fig. 6; Supporting Information Table S9). Total number of genera identified increased each year of our study (5, 7, and

Table 1. Light transmittance and attenuation coefficients (K_D) of ice and the water column on South Sparkling Bog in Year 3: black ice. A single ice K_D was calculated for all dates.

		PAR (μmol m^{-2} s^{-1})			K_D (m^{-1})	
Date	Ice (m)	Surface	Under ice	Transmittance (%)	Ice	Water
13 Jan 2021	0.28	904.00	109.20	0.12	4.45	2.65
02 Feb 2021	0.38	367.40	58.76	0.16	4.45	2.54
02 Mar 2021	0.59	1442.00	227.60	0.16	4.45	4.24
15 Mar 2021	0.47	1136.00	366.50	0.32	4.45	1.65

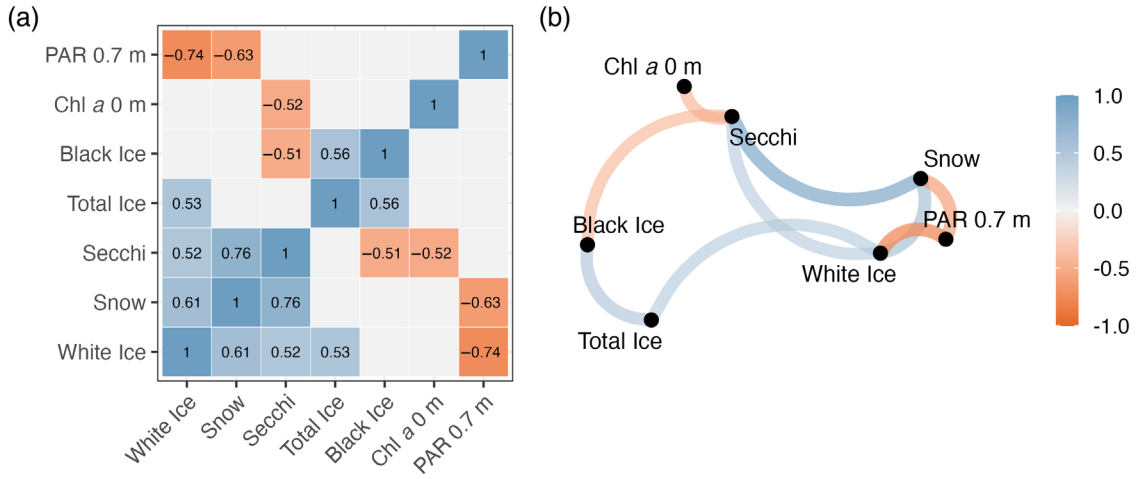

Fig. 4. (**a**) Correlation matrix for South Sparkling Bog environmental variables. Correlations with $p < 0.10$ are shown in blue/red, with the corresponding correlation coefficient. PAR data have been $\log_{10}$ transformed. (**b**) Correlation network plot for the environmental variables with significant correlations.

10, respectively). Zooplankton species richness was greatest at 10 in Year 2. Years 1 and 3 had species richness values of 4 and 5, respectively. Zooplankton Shannon genera diversity values ranged from 0.60 (March 2020) to 1.41 (March 2019) and varied across all sampling dates and appeared to slightly decline in snow-removal years (Supporting Information Fig. S1).

Overall, rotifers accounted for 99.4% of total winter zooplankton abundance (Fig. 6). The Cladocera suborder accounted for 0.6% of zooplankton observed. The subclass Copepoda were not observed in any winter zooplankton samples through the duration of this study. Within the phylum Rotifera, we observed specimens of both Monogononta and Bdelloidea classes. Bdelloidea rotifers were unidentifiable beyond class rank due to sample preservation. All rotifers identified to the genus level were within the Monogononta class and dominated the zooplankton community, accounting for 78.2% of the study total abundance. Class Bdelloidea only contributed 5.4% of overall abundance, and the remaining 15.8% of zooplankton were unidentifiable rotifers. When zooplankton were grouped based on trophi structure, the community could be separated into five groupings: virgate trophi 1 and 2, incudate trophi, malleate trophi, and other (N/A, accounts for all non-Monogononta organisms).

Zooplankton densities increased in both snow removal years (Fig. 6); however, Year 2 densities were more similar to Year 1 than Year 3. Maximum densities by year were: 2019 = 0.127 individuals L^{-1}, 2020 = 0.846 individuals L^{-1}, and 2021 = 70.2 individuals L^{-1}. Year 3 was dominated by the genera *Ascomorpha* and *Asplanchna* (Fig. 6a,b). The virgate trophi 1 group was only present in the snow removal years, and it had the highest densities during Year 3 (Fig. 6c,d). All other trophi groups were present in all years. Grouping both by genus and trophi groupings, ANOSIM tests revealed significant ($p < 0.05$) differences between zooplankton total densities between years, but not relative abundance (Table 2).

Constrained ordination

RDA plots reveal the environmental conditions that were correlated to phytoplankton community composition across the 3 yr of study. In the model grouped by division, the overall model had an adjusted r^2 of 0.50 (Supporting Information Table S7). The first RDA axis was significant, provided most (64.8%) of the explanatory value, and was positively related to PAR and black ice, and negatively related to white ice thickness and Secchi depth (Fig. 7a). In the model grouped by morphofunctional group, the overall model had an adjusted r^2 of 0.40, and the explanatory variables positioned similarly along Axis 1 (significant, 40.6% of variance). In ANOVA permutation tests of both models, only PAR at 0.7 m was significant in both models ($p < 0.05$; Supporting Information Table S7). All other terms were not significant. Overall, Chlorophyta and Cyanophyta abundance and total phytoplankton biovolume were all positively correlated to PAR and black ice thickness, whereas Chrysophyta density was positively correlated to white ice thickness. Abundance of Chlorophytes was most positively correlated to PAR and black ice thickness, whereas large mixotrophs were most positively associated with low PAR and thick white ice (Fig. 7b).

CCA plots reveal the environmental conditions that were correlated to zooplankton community composition across the 3 yr of study (Fig. 7c,d). When zooplankton were grouped by genera, the environmental variables that grouped closely together included: (1) white ice thickness and Cyanophyta biovolume; and (2) Chlorophyta biolvolume, total phytoplankton biovolume, and black ice thickness. All terms except for total phytoplankton biovolume were significant at $p < 0.05$ (Supporting Information Table S7). *Ascomorpha* was more likely to be present under white ice conditions with Cyanophyta, whereas *Asplancha* was more likely to be present under black ice conditions with Chlorophyta (Fig. 7c).

Grouping zooplankton communities into trophi structure groups provided a higher level of interpretability based on

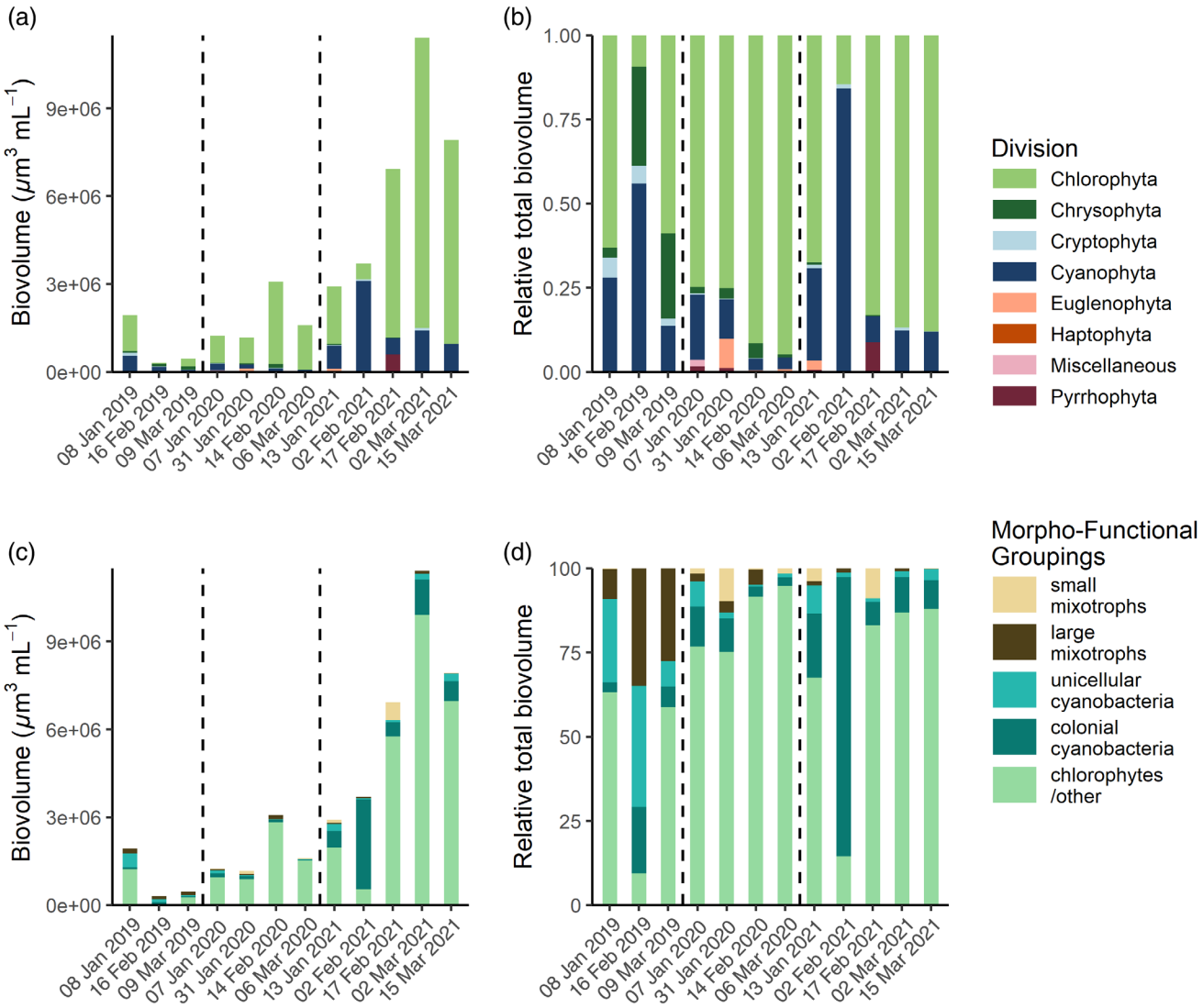

Fig. 5. South Sparkling Bog phytoplankton division grouping for (**a**) total biovolume and (**b**) relative biovolume for each winter sampling date. (**c**) Phytoplankton morphofunctional groupings for (**c**) total biolvolume and (**d**) relative biovolume for each winter sampling date. Groupings are based on Salmaso and Padisák (2007).

Table 2. Statistical results (*p*-value and *R*) from ANOSIM tests on phytoplankton and zooplankton community composition between the 3 yr. *R* is constrained between −1 to 1, with *R* close to 1 suggesting dissimilarity between groups.

Community parameter	Grouping	*p*-value	ANOSIM *R* statistic
Phytoplankton biovolume	Division	$p = \mathbf{0.008}$	$R = 0.46$
Phytoplankton biovolume	Morphofunctional groupings	$p = \mathbf{0.002}$	$R = 0.49$
Phytoplankton relative biovolume	Division	$p = 0.07$	$R = 0.19$
Phytoplankton relative biovolume	Morphofunctional groupings	$p = \mathbf{0.047}$	$R = 0.25$
Zooplankton total density	Genus	$p = \mathbf{0.002}$	$R = 0.79$
Zooplankton total density	Trophi groupings	$p = \mathbf{0.002}$	$R = 0.72$
Zooplankton relative abundance	Trophi genus	$p = 0.117$	$R = 0.18$
Zooplankton relative abundance	Trophi groupings	$p = 0.667$	$R = -0.08$

Significant *p*-values ($p < 0.05$) are bolded.

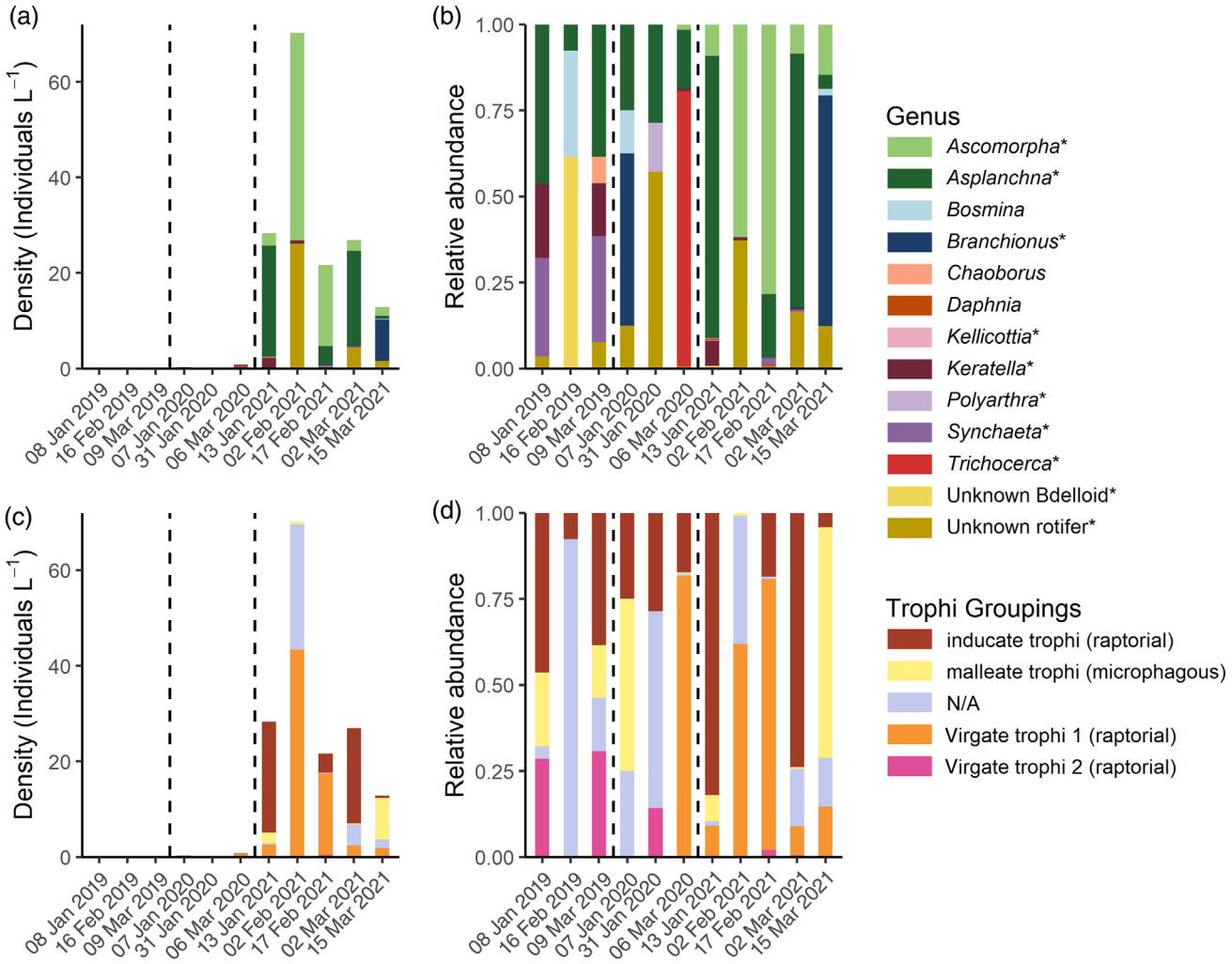

Fig. 6. South Sparkling Bog zooplankton grouping by genera for (**a**) density and (**b**) relative abundance for each winter sampling date. Rotifer taxa are distinguished with an asterisk. Zooplankton trophi groupings for (**c**) density and (**d**) relative abundance. Groupings are based on Oh et al. (2017).

percent variance explained (CCA1 = 50.0%, CCA2 = 29.2%). Based on trophi structure functional groupings, the most significant explanatory variable was Chlorophyta biovolume (Supporting Information Table S8). The CCA for trophi groupings shows that malleate (or the microphagous rotifers found in this study) were found when black : white ice thickness was high. Virgate trophi groups (1 and 2) were driven by different environmental variables. Virgate trophi 1 zooplankton abundance was greater under conditions with higher Cyanophyta biovolumes and white ice. Virgate trophi 2 groups were not related to phytoplankton composition (Fig. 7d).

Discussion

Our snow removal efforts were partially successful in changing the ice characteristics and light environment on South Sparkling Bog (Fig. 8). Comparing between years, the changes in underwater PAR in South Sparkling Bog were due to a combination of snow removal and the thickness of white and black ice. Through snow removal, we effectively removed the reflective properties of the overlying snow, and created an environment that allowed greater light penetration into the lake ice. By removing snow, we also prevented the further formation of white ice. However, if white ice was formed during initial ice-formation (as in Year 2), it persisted. The snow and ice thicknesses across our three study years suggest that white ice thickness > 10.5 cm inhibits appreciable light transmission. Aside from 06 March 2020, all sampling dates in Years 1 and 2 had white ice thicknesses greater than 10.5 cm, which attenuated almost all light (Fig. 2). In Year 3, white ice thickness never exceeded 10.5 cm, and maximum PAR in the water column was reached after 02 March 2021, during which there was no snow and ≤ 8 cm of white ice (Figs. 2, 3). Keeping in mind, sun angle and maximum surface PAR are rapidly increasing from January through March, light transmission through the ice-cover also increased from 12% to 32% over

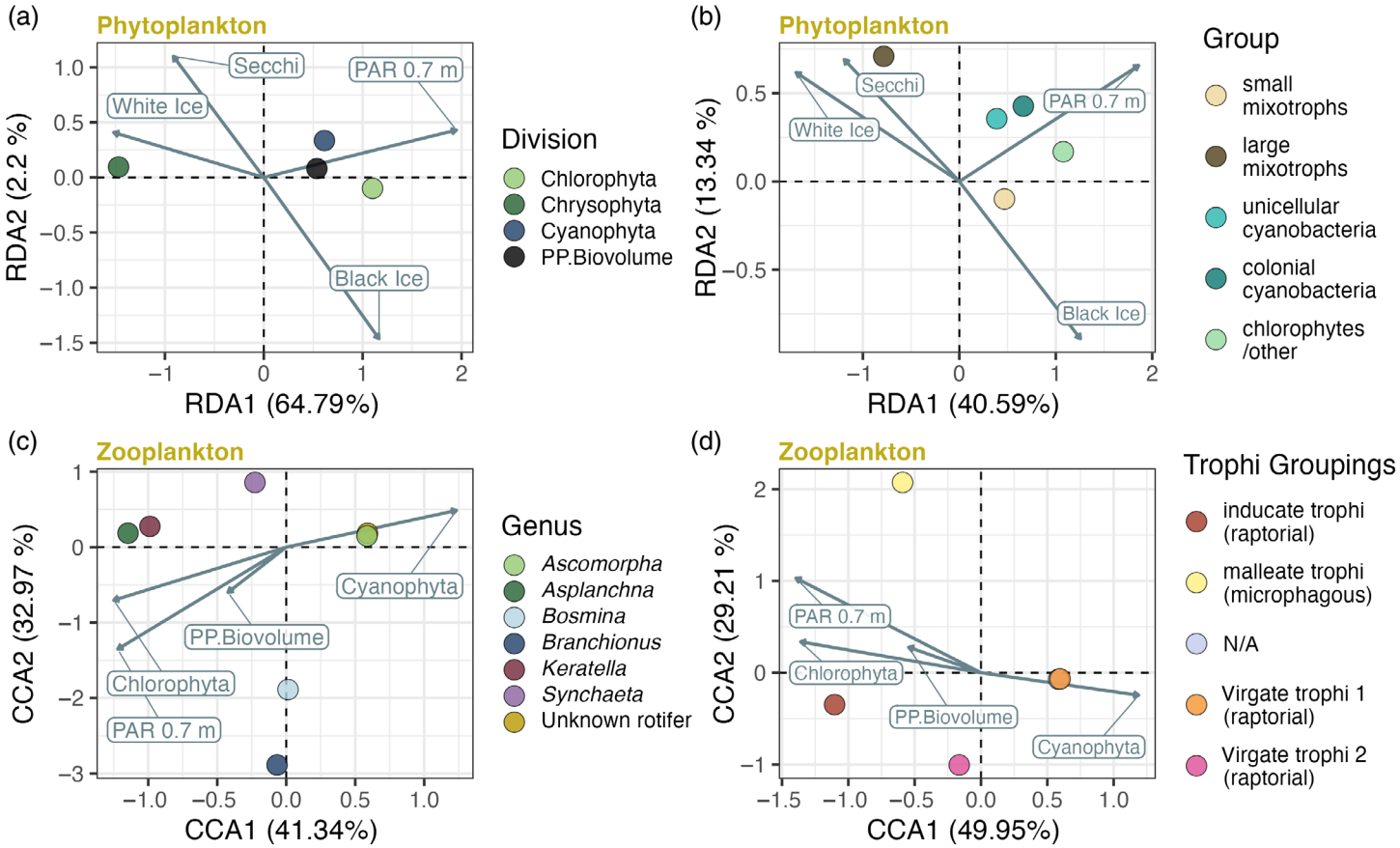

Fig. 7. Biplot of the first two axes from the phytoplankton RDAs of (**a**) density of Cyanophyta and Chlorophyta and total phytoplankton biovolume and (**b**) morphofunctional group. (**c**) Biplot of the first two axes from the zooplankton CCAs grouped by (**c**) genus and (**d**) trophi group. In (**c**) only genera observed on three or more sampling days were used in the model. The percent explained by each axis is reported on the axis label.

this period (Table 1). Our ice transmission percentages fall between those measured on oligotrophic (21.4–38.5%) and dystrophic (0.5–4.7%) Minnesota lakes (Bramburger et al. 2022). Similarly, our ice K_d of 4.45 was greater than the Minnesota oligotrophic lakes (K_d: 1.24–2.49) and less than the dystrophic lakes (K_d: 6.54–8.10) (Bramburger et al. 2022).

Observed increases in both surface and mean Chl *a* concentrations and phytoplankton biovolume confirm increases in photosynthetic primary production during snow removal years (Figs. 2c, 5) even at extremely low PAR. Only in Year 3 did mean PAR exceed 7.6 μmol m^{-2} s^{-1}, and maximum PAR exceed 20 μmol m^{-2} s^{-1}, values that have been cited as the minimum PAR required for photosynthesis and the minimum PAR required for biomass accumulation, respectively (Gosselin et al. 1985; Pernica et al. 2017). Although these thresholds do correspond to a large increase in phytoplankton biovolume in Year 3, in Years 1 and 2 there is evidence that photosynthesis is taking place when mean daily PAR is < 7.6 μmol m^{-2} s^{-1}. This value is lower than the range of mean daily mixed layer irradiance (E24) thresholds for light limitation found in ice-covered Canadian lakes (34.7–41.7 μmol m^{-2} s^{-1}; Dubourg et al. 2015). These findings emphasize the need for more empirical studies establishing the relationship between PAR, Chl *a*, and phytoplankton biomass in low-light conditions, and between lakes of different trophic states. In addition, our finding of increased phytoplankton biomass with increasing PAR is different than previous short-term snow removal experiments, where researchers found that phytoplankton acclimated to low-light environments showed diminished photosynthetic efficiency when irradiance was suddenly increased (Jewson et al. 2009; Garcia et al. 2019; Bramburger et al. 2022). Our experiment is one of the first to sustain snow-free conditions, and therefore our findings are more realistic of long-term environmental change, where community composition is a reflection of long-term conditions.

Mixotrophs and potential mixotrophs had their greatest relative biovolume in Year 1, when light availability under ice was almost unmeasurable (Fig. 5). Mixotrophic groups were most correlated by environmental variables that are proxies for a low-light environment (Fig. 7b). In addition, nearly all mixotrophs were motile (Supporting Information Table S4).

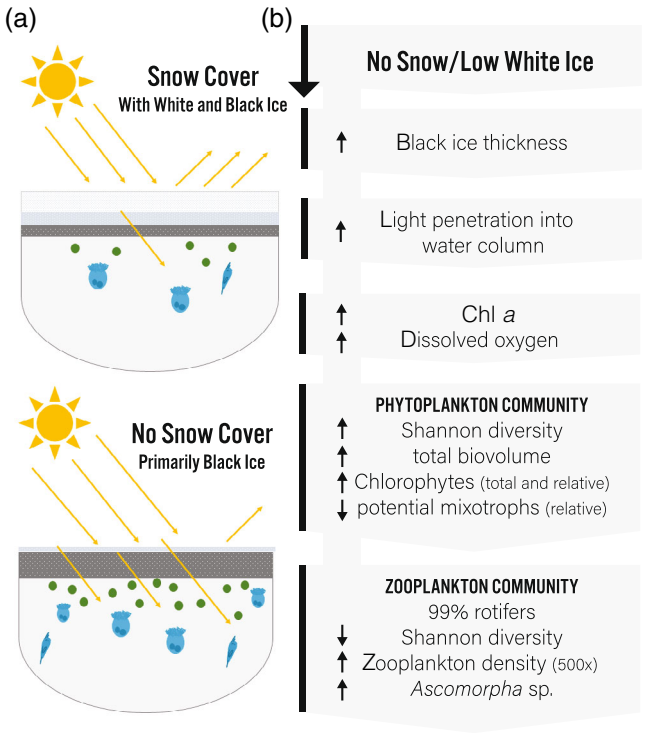

Fig. 8. (**a**) Illustrated depiction of the outcomes of the snow manipulation on the physical environment and biological communities in South Sparkling Bog. (**b**) Flowchart of major biotic results following snow removal on South Sparkling Bog and subsequent changes to under-ice characteristics in 2021.

These results corroborate previous research asserting that successful phytoplankton taxa under low-light conditions typically have adaptations allowing for mixotrophy and/or motility (flagellated; Özkundakci et al. 2016). Therefore, our community composition of phytoplankton in the reference year that was marked by light limitation, aligns with expectations that mixotrophs should account for most of the phytoplankton community (Sanders et al. 1990).

In the snow removal years, the total and relative biovolume of the division Chlorophyta markedly increased. Chlorophytes became the dominant phytoplankton group in both snow-removal years. Green algae are generally better adapted to high light environments (Schwaderer et al. 2011). Chlorophytes are photosynthetic autotrophs and cannot rely on heterotrophic processes to obtain energy when light is limited. For Chlorophytes, the availability of PAR can determine their spatial distribution and utilization of starch reserves when light is low (Bielewicz et al. 2011). Therefore, increases in light availability during manipulation years explain the observed increase in Chlorophyta. Chlorophytes primarily composed the morph-functional group of large, non-flagellated, unicellular phytoplankton (group "other"). Our inference that light influenced the greater biovolume of Chlorophytes is supported by the results of the RDA (Fig. 7a,b). Higher PAR and black ice thickness were the environmental variables that positively correlated with this grouping. Therefore, we deduce that the changes in PAR under ice, as driven by the snow removal, promoted Chlorophyte growth, and resulted in overall higher phytoplankton biomass and a Chlorophyte dominated phytoplankton community in manipulation years.

Despite light limitations, diatoms are often a dominant group in winter phytoplankton communities, as many species are well adapted to cold water and can proliferate in low-light conditions (Kong et al. 2021). Although diatom species are present in open-water South Sparkling Bog samples, we did not observe any diatoms in the winter samples. We think this may be related to sinking factors (Ferris and Lehman 2007), as diatoms were not silica limited (Supporting Information Table S3). In the limited studies that report finding few to no diatom species in small, humic lakes, is it thought they are unable to maintain buoyancy in the water column, and settle out due to low turbulence in the shallow photic zone (Jones 1998).

Cyanophytes were equally abundant in Years 1 and 3 (Fig. 5). Under lake ice, Cyanophytes can persist and even dominate winter phytoplankton communities. Some research suggests that certain Cyanophytes favor lower temperatures, thicker ice, and very little oxygen (Babanazarova et al. 2013). However, other research that explores phytoplankton communities under ice has attributed increases in Cyanophytes, in part, to milder winter conditions like increased light and shorter ice cover duration (Dokulil and Herzig 2009). In contrast, Özkundakci et al. (2016) observed little-to-no change in Cyanophytes based on winter severity and ice thickness. Our RDA revealed that Cyanophytes were positively correlated with a higher light environment, but less so than Chlorophytes (Fig. 7). Because under-ice Cyanophyte characteristics seem to vary across study systems, winter severity, and community composition, we attribute the minor observed increase in Cyanophyte relative biovolume to taxa-specific traits like light tolerance ranges and light harvesting efficiency. Across all sampling dates, the dominant Cyanophytes genera (in terms of biovolume) were *Aphanocapsa* sp. and *Aphanothece* sp. These picophytoplankton are known to thrive under a wide range of light availability and can even boost productivity under low-light conditions (Gupta and Agrawal 2006; Magalhães et al. 2019). This may explain similar yet slight differences in abundance between sampling years.

Zooplankton communities under lake ice are typically dominated by copepods and rotifers (Blank et al. 2009; Perga et al. 2021). However, we did not observe a single copepod in the under-ice samples from South Sparkling Bog, even when nauplii and adult copepods were present in fall and spring zooplankton samples. Though many copepods actively overwinter, many employ diapause strategies. In general, adult and late-stage juveniles remain in the deeper waters near the

sediments, while nauplii are distributed nearer to the surface and water–ice interface (Perga et al. 2021). It is unlikely that our sampling protocol was unable to capture deep zooplankton, as a lack of oxygen in the water column below 2 m renders most of the water column uninhabitable. We assume the absence of nauplii in surface waters may be due to lack of reproduction and hatching.

The phylum Rotifera, and specifically the Monogononta class, dominated all zooplankton samples (Fig. 6). The life history traits and evolutionary adaptations of many rotifers allow them to thrive under ice. Rotifers are generally small, have short life cycles, and can reproduce very quickly, allowing them to respond quickly to environmental change (Gyllström and Hansson 2004). In addition, many groups have adaptations that are well suited for harsher or more extreme conditions. Many rotifers that proliferate in cold, under-ice environments are cold-stenothermal species (Virro et al. 2009). Studies suggest that cold-stenothermal rotifers require an oxygen-rich environment (Bērziņš and Pejler 1989). Although we measured little-to-no oxygen during all study winters (Fig. 3), it is possible that oxygen concentrations increased closer to the water–ice interface, where primary production is most abundant in the photic zone. Some zooplankton can tolerate low-oxygen and anoxic conditions (Karpowicz et al. 2020); however, the development of rotifers is often limited by the effects of temperature and oxygen (Herzig 1987).

If we examine the NTL-LTER long-term data of the winter zooplankton community in a nearby dystrophic bog lake, Trout Bog, we see a link between zooplankton density and dissolved oxygen saturation (Supporting Information Fig. S2). Zooplankton densities decline significantly in the same years the dissolved oxygen saturation drops below 5%. The availability of dissolved oxygen in the water column of South Sparkling Bog might explain the observed trends in zooplankton densities. Both snow removal years had greater zooplankton densities than Year 1. However, in the Year 2, zooplankton densities were more similar to Year 1, while in Year 3 densities rose by two orders of magnitude, from a maximum of 0.127 individuals per liter in February 2019 to 70.2 individuals per liter in February 2021. The higher zooplankton densities in Year 3 coincide with higher phytoplankton densities. More primary production in the water column would support zooplankton biomass in two ways: (1) directly through increased food availability, and (2) indirectly through oxygen production. While our measurements of dissolved oxygen via a high-frequency sensor at 0.70 m depth did not record the presence of oxygen until late March in the manipulation years (Fig. 3), it may be that a very shallow oxic layer existed directly below the ice. This result speaks to the difficulty of sensor deployment that is able to capture habitat characteristics at the ice/water interface while not being frozen into the ice as the ice cover thickens. It also speaks to the difference in under-ice habitat available for zooplankton in dystrophic lakes that tend to have extremely high rates of oxygen consumption (Shade et al. 2012), vs. oligotrophic lakes that often have ample oxygen available throughout most of the water column (Powers et al. 2017) and support higher densities of crustacean zooplankton under ice (Hampton et al. 2017).

In other studies of zooplankton community composition under lake ice, timing of ice onset has been found to be a possible driver of zooplankton density. Specifically, research suggests that later ice onset promotes greater survival of overwintering species, likely due to increased time to accumulate nutritional fatty acids and prolonged primary production in the fall that is not limited by ice cover (Hébert et al. 2021). Given the similarity in timing of ice-onset in our study (10 d; Supporting Information Table S2), we do not think ice duration played a role in structuring phytoplankton and zooplankton composition.

Based on the CCA analysis, the environmental variables that most strongly explained the variation in the zooplankton community (based on trophi groupings) were mean daily PAR at 0.7 m, Chlorophyta biovolume, and Cyanophyte biovolume (Supporting Information Table S8), and seem to have differentially impacted both the microphagous (*Branchionus* sp., *Kellicottia* sp., and *Keratella* sp.) and raptorial (*Ascomorpha* sp., *Asplanchna* sp., *Polyarthra* sp., *Synchaeta* sp., and *Trichocerca* sp.) rotifers in our samples. Studies that investigate the functional traits of rotifers in relation to various environmental variables are increasing. Many of these studies investigate how lake trophic status impacts various traits, with many finding that microphagous rotifers dominate in more productive lakes. Similarly, microphagous feeders, and especially the malleate trophi group, have been associated with higher chlorophyll concentrations (Oh et al. 2017; Wang et al. 2022). Our results show that microphagous feeders were positively correlated with PAR at 0.7 m, Chlorophyte biovolume, and total primary producer biovolume, and they were most abundant when water column Chlorophyll concentrations were relatively high, potentially suggesting that the increased light under ice promoted food availability for this functional group.

In contrast, raptorial feeders have been found to coexist with their competitors, and the virgate trophi especially promotes a diversity of food intake under competitive conditions (Wang et al. 2022). This is because the virgate trophi consume many smaller food items in addition to the the large, single food particles that raptorial feeders typically prefer to eat (Obertegger and Manca 2011). We believe that observed correlations between raptorial rotifers and environmental variables can be further explained by individual taxonomic traits.

Ascomorpha sp. (virgate trophi 1, raptorial feeder) were dominant genera, and were most abundant in Year 3 (Fig. 6). *Ascomorpha* sp. are known to consume large, unicellular phytoplankton, often exclusively dinoflagellates (Stelzer 1998). Year 3 also saw the highest abundance of dinoflagellates; however, it is unlikely that dinoflagellates were abundant enough to solely sustain the *Ascomorpha* sp. population. Our CCA

analysis shows that *Ascomorpha* sp. (and the virgate trophi 1 group) were also highly correlated with Cyanophyta biovolume. Although Cyanophytes are generally believed to be poor in nutritional quality for zooplankton, our results suggest that *Ascomorpha* sp. were likely feeding directly on, or indirectly subsisting on, Cyanophytes through an intermediate trophic level. Specifically, new research suggests that micrograzers (e.g., ciliates) can be key intermediate trophic levels responsible for transferring energy from Cyanophytes to rotifers (Sweeney et al. 2022). Although we did not investigate micrograzers in this study, they may be important players in explaining the high correlation between Cyanophytes and both *Ascomorpha* sp. and the virgate trophi 1 group.

The genus, *Asplanchna* (incudate trophi group, raptorial feeder), was another dominant taxa and the only zooplankton genus that was present in nearly every sampling event (Fig. 6). *Asplanchna brightwelli* and *Asplanchna priodonta* were the two identifiable *Asplanchna* species found in this study. Although they are omnivorous, *A. brightwelli* is often a predator to other rotifer species and commonly feeds on genera like *Keratella* and *Branchionus* (Sarma et al. 1997). *A. priodonta* is usually omnivorous supplementing its rotifer diet with colonial algae and even cyanobacteria (Kappes et al. 2000). The observed increases in *Asplanchna* sp. populations in Year 3 are likely explained by feeding habits, as both their potential food sources (phytoplankton and rotifer prey) also increased during this year.

Future directions

Because the light-limited environment created by snow and ice cover presents limitations to primary production and dietary challenges to overwintering zooplankton in lakes, there is a growing body of research that explores energy acquisition through heterotrophic processes, energy storage strategies, and feeding behavior. Species-specific strategies of lipid accumulation (from phytoplankton) during autumn and early winter have been found to be integral in active overwintering by some species (Grosbois et al. 2017). Specifically, when starved, *Leptodiaptomus minutus* depended on fatty acids accumulated from phytoplankton to maintain metabolic functioning and reproduction (Grosbois et al. 2017). When light limits primary production and reduces grazing opportunities, zooplankton can obtain energy from sources that are not phytoplankton derived. Research suggests that when primary production is low, some zooplankton use allochthonous organic carbon sources (Rautio et al. 2011). These mechanisms are relevant in humic lakes where high DOC concentrations rapidly attenuate light in the water column and limit primary production. In addition, many zooplankton that successfully over winter rely on fatty acid storages that were accumulated in the autumn, prior to ice-onset (Hébert et al. 2021). Future studies of this kind should sample the nutritional quality of phytoplankton and fatty acid storages of zooplankton prior to ice-on and through the duration of ice cover. This information will be useful in understanding zooplankton winter feeding habits, and the relationship between increased phytoplankton production and zooplankton population dynamics.

Dissolved oxygen is also a critical habitat constraint that can determine and exclude the presence and proliferation of certain grazer species. While measured dissolved oxygen levels remained extremely low in this study, future work should employ micoprofile sampling near the surface. During periods of ice cover, primary production typically occurs near the very surface of the water column (Yoshida et al. 2003). In marine environments, there are many observations of phytoplankton adhering to the under-side of ice, although the availability of microhabitats is likely less in hard freshwater ice than in soft marine ice with plentiful brine channels (Castellani et al. 2022). Our surface level measurements for dissolved oxygen were at a depth of 0.7 m. Although this depth was relatively close to the water–ice interface, obtaining a more fine-scale depth resolution, especially within the photic zone, may offer more insights to the role of winter oxygen level in structuring the presence and distribution plankton communities under ice.

Conclusion

Warming air temperature from climate change is resulting in declining coverage and duration of lake ice globally. Coupled with less lake ice, projected changes to winter precipitation patterns will alter the standing snow cover on many lakes, especially those in mid- to north-temperate climates that are situated close the transitional zone of intermittent lake ice. To predict how changing winter weather will impact lake ecosystems, it is essential that we understand the feedbacks between lake physics and biological communities under ice. In terms of under-ice plankton research, this study is unique in its focus on a dystrophic system, as well as its sampling resolution and frequency (Chiapella et al. 2021). In this study, we employed a multiyear snow manipulation with the goal of altering under-ice light availability. Our snow removal efforts were successful, and we observed increases in phytoplankton biovolume, photoautotroph relative biovolume, and consumer densities, alongside increases to PAR. Furthermore, many changes in specific plankton taxa and groups could be explained by changes to the light environment.

Studying how biological communities might respond to changing winters in dystrophic systems is important, as we know lakes are experiencing browning worldwide (Williamson et al. 2016; Meyer-Jacob et al. 2019). In terms of food webs, darkening and browning can potentially shift grazer community structure to favor large-bodied species while altering trophic interactions between planktivorous fish, invertebrate predators, and grazers (Wissel et al. 2003). Changes to plankton communities and trophic interactions have the potential to alter lake phenology (Sommer and Lewandowska 2011; Sharma et al. 2021), create mismatch events (de Senerpont

Domis et al. 2007), and scale up to impact global nutrient and carbon cycling (Schmitz et al. 2014).

Data availability statement

Zooplankton data are available at: https://doi.org/10.6073/pasta/f6e271634a04819e25bc7c913cd67155. Phytoplankton data are available at: https://doi.org/10.6073/pasta/f6e271634a04819e25bc7c913cd67155. Ice, snow, and Secchi data are available at: https://doi.org/10.6073/pasta/962fa57959ff9828eb6f1cbda79b82c0.

References

Allan, J. D. 1977. An analysis of seasonal dynamics of a mixed population of *Daphnia*, and the associated cladoceran community. Freshw. Biol. **7**: 505–512. doi:10.1111/j.1365-2427.1977.tb01701.x

Ariano, S. S., and L. C. Brown. 2019. Ice processes on medium-sized north-temperate lakes. Hydrol. Process. **33**: 2434–2448. doi:10.1002/hyp.13481

Arndt, S., K. M. Meiners, R. Ricker, T. Krumpen, C. Katlein, and M. Nicolaus. 2017. Influence of snow depth and surface flooding on light transmission through Antarctic pack ice. J. Geophys. Res. Oceans **122**: 2108–2119. doi:10.1002/2016JC012325

Babanazarova, O., S. Sidelev, and S. Schischeleva. 2013. The structure of winter phytoplankton in Lake Nero, Russia, a hypertrophic lake dominated by Planktothrix-like Cyanobacteria. Aquat. Biosyst. **9**: 18. doi:10.1186/2046-9063-9-18

Bērziņš, B., and B. Pejler. 1989. Rotifer occurrence in relation to oxygen content. Hydrobiologia **183**: 165–172. doi:10.1007/BF00018721

Bielewicz, S., E. Bell, W. Kong, I. Friedberg, J. C. Priscu, and R. M. Morgan-Kiss. 2011. Protist diversity in a permanently ice-covered Antarctic Lake during the polar night transition. ISME J. **5**: 1559–1564. doi:10.1038/ismej.2011.23

Blank, K., J. Haberman, M. Haldna, and R. Laugaste. 2009. Effect of winter conditions on spring nutrient concentrations and plankton in a large shallow Lake Peipsi (Estonia/Russia). Aquat. Ecol. **43**: 745–753. doi:10.1007/s10452-009-9283-2

Bramburger, A. J., T. Ozersky, G. M. Silsbe, C. J. Crawford, L. G. Olmanson, and K. Shchapov. 2022. The not-so-dead of winter: Underwater light climate and primary productivity under snow and ice cover in Inland Lakes. Inland Waters **1–19**: 1–12. doi:10.1080/20442041.2022.2102870

Castellani, G., and others. 2022. Shine a light: Under-ice light and its ecological implications in a changing Arctic Ocean. Ambio **51**: 307–317. doi:10.1007/s13280-021-01662-3

Cavaliere, E., and others. 2021. The lake ice continuum concept: Influence of winter conditions on energy and ecosystem dynamics. J. Geophys. Res. Biogeosci. **126**: 1-19. doi:10.1029/2020JG006165

Chiapella, A. M., H. Grigel, H. Lister, A. Hrycik, B. P. O'Malley, and J. D. Stockwell. 2021. A day in the life of winter plankton: Under-ice community dynamics during 24 h in a eutrophic lake. J. Plankton Res. **43**: 865–883. doi:10.1093/plankt/fbab061

Choi, G., D. A. Robinson, and S. Kang. 2010. Changing Northern Hemisphere snow seasons. J. Climate **23**: 5305–5310. doi:10.1175/2010JCLI3644.1

de J. Magalhães, A. A., L. D. da Luz, and T. R. de Aguiar Junior. 2019. Environmental factors driving the dominance of the harmful bloom-forming cyanobacteria Microcystis and Aphanocapsa in a tropical water supply reservoir. Water Environ. Res. **91**: 1466–1478. doi:10.1002/wer.1141

de Senerpont Domis, L. N., W. M. Mooij, S. Hülsmann, E. H. van Nes, and M. Scheffer. 2007. Can overwintering versus diapausing strategy in *Daphnia* determine match–mismatch events in zooplankton-algae interactions? Oecologia **150**: 682–698. doi:10.1007/s00442-006-0549-2

Dokulil, M. T., and A. Herzig. 2009. An analysis of long-term winter data on phytoplankton and zooplankton in Neusiedler See, a shallow temperate lake, Austria. Aquat. Ecol. **43**: 715–725. doi:10.1007/s10452-009-9282-3

Dubourg, P., R. L. North, K. Hunter, D. M. Vandergucht, O. Abirhire, G. M. Silsbe, S. J. Guildford, and J. J. Hudson. 2015. Light and nutrient co-limitation of phytoplankton communities in a large reservoir: Lake Diefenbaker, Saskatchewan, Canada. J. Great Lakes Res. **41**: 129–143. doi:10.1016/j.jglr.2015.10.001

Ferris, J. A., and J. T. Lehman. 2007. Interannual variation in diatom bloom dynamics: Roles of hydrology, nutrient limitation, sinking, and whole lake manipulation. Water Res. **41**: 2551–2562. doi:10.1016/j.watres.2007.03.027

Garcia, S. L., A. J. Szekely, C. Bergvall, M. Schattenhofer, and S. Peura. 2019. Decreased snow cover stimulates under-ice primary producers but impairs methanotrophic capacity. mSphere **4**: e00626-18. doi:10.1128/mSphere.00626-18

Gosselin, M., L. Legendre, S. Demers, and R. G. Ingram. 1985. Responses of sea-ice microalgae to climatic and fortnightly tidal energy inputs (Manitounuk Sound, Hudson Bay). Can. J. Fish. Aquat. Sci. **42**: 999–1006. doi:10.1139/f85-125

Grosbois, G., H. Mariash, T. Schneider, and M. Rautio. 2017. Under-ice availability of phytoplankton lipids is key to freshwater zooplankton winter survival. Sci. Rep. **7**: 11543. doi:10.1038/s41598-017-10956-0

Grosbois, G., and M. Rautio. 2018. Active and colorful life under lake ice. Ecology **99**: 752–754. doi:10.1002/ecy.2074

Gupta, S., and S. C. Agrawal. 2006. Survival of blue-green and green algae under stress conditions. Folia Microbiol. **51**: 121–128. doi:10.1007/BF02932166

Gyllström, M., and L.-A. Hansson. 2004. Dormancy in freshwater zooplankton: Induction, termination and the importance of benthic-pelagic coupling. Aquat. Sci. **66**: 274-295. doi:10.1007/s00027-004-0712-y

Grolemund, G. and H. Wickham (2011). Dates and times made easy with lubridate. J. Stat. Softw., **40**: 1-25. Available from https://www.jstatsoft.org/v40/i03/

Hampton, S. E., and others. 2017. Ecology under lake ice. Ecol. Lett. **20**: 98–111. doi:10.1111/ele.12699

Hébert, M.-P., B. E. Beisner, M. Rautio, and G. F. Fussmann. 2021. Warming winters in lakes: Later ice onset promotes consumer overwintering and shapes springtime planktonic food webs. Proc. Natl. Acad. Sci. **118**: e2114840118. doi:10.1073/pnas.2114840118

Herzig, A. 1987. The analysis of planktonic rotifer populations: A plea for long-term investigations, p. 163–180. *In* L. May, R. Wallace, and A. Herzig [eds.], Rotifer Symposium IV. Springer Netherlands. doi:10.1007/978-94-009-4059-8_22

Hrycik, A. R., and others. 2021. Earlier winter/spring runoff and snowmelt during warmer winters lead to lower summer chlorophyll-*a* in north temperate lakes. Glob. Chang. Biol. **27**: 4615–4629. doi:10.1111/gcb.15797

Hrycik, A. R., and J. D. Stockwell. 2021. Under-ice mesocosms reveal the primacy of light but the importance of zooplankton in winter phytoplankton dynamics. Limnol. Oceanogr. **66**: 481–495. doi:10.1002/lno.11618

Imrit, M. A., and S. Sharma. 2021. Climate change is contributing to faster rates of Lake ice loss in lakes around the Northern Hemisphere. J. Geophys. Res. Biogeo. **126**: 1–13. doi:10.1029/2020JG006134

Jewson, D. H., N. G. Granin, A. A. Zhdanov, and R. Y. Gnatovsky. 2009. Effect of snow depth on under-ice irradiance and growth of *Aulacoseira baicalensis* in Lake Baikal. Aquat. Ecol. **43**: 673–679. doi:10.1007/s10452-009-9267-2

Jones, R. I. 1998. Phytoplankton, primary production and nutrient cycling, p. 145–175. *In* M. M. Caldwell, G. Heldmaier, O. L. Lange, H. A. Mooney, E.-D. Schulze, U. Sommer, D. O. Hessen, and L. J. Tranvik [eds.], Aquatic humic substances, v. **133**. Springer Berlin Heidelberg. doi:10.1007/978-3-662-03736-2_8 Series title: Ecological studies.

Kalinowska, K., and M. Grabowska. 2016. Autotrophic and heterotrophic plankton under ice in a eutrophic temperate lake. Hydrobiologia **777**: 111–118. doi:10.1007/s10750-016-2769-8

Kappes, H., C. Mechenich, and U. Sinsch. 2000. Long-term dynamics of *Asplanchna priodonta* in Lake Windsborn with comments on the diet. Hydrobiologia **432**: 91–100. doi:10.1023/A:1004022020346

Karpowicz, M., J. Ejsmont-Karabin, J. Kozlowska, I. Feniova, and A. R. Dzialowski. 2020. Zooplankton community responses to oxygen stress. Water **12**: 706. doi:10.3390/w12030706

Katz, S. L., L. R. Izmest'eva, S. E. Hampton, T. Ozersky, K. Shchapov, M. V. Moore, S. V. Shimaraeva, and E. A. Silow. 2015. The "Melosira years" of Lake Baikal: Winter environmental conditions at ice onset predict under-ice algal blooms in spring. Limnol. Oceanogr. **60**: 1950–1964. doi:10.1002/lno.10143

Kong, X., M. Seewald, T. Dadi, K. Friese, C. Mi, B. Boehrer, M. Schultze, K. Rinke, and T. Shatwell. 2021. Unravelling winter diatom blooms in temperate lakes using high frequency data and ecological modeling. Water Res. **190**: 116681. doi:10.1016/j.watres.2020.116681

Kuhn, M., S. Jackson, and J. Cimentada (2020). corrr: Correlations in R. R package version 0.4.4. Available from https://CRAN.R-project.org/package=corrr

Lemke, P., and others. 2007. Observations: Changes in snow, ice and frozen ground, p. 337–383. *In* Climate change 2007: The physical science basis. Contribution of Working Group I to the Fourth Assessment Report of the Intergovernmental Panel on Climate Change. Cambridge Univ. Press.

Lenard, T., and W. Ejankowski. 2017. Natural water brownification as a shift in the phytoplankton community in a deep hard water lake. Hydrobiologia **787**: 153–166. doi:10.1007/s10750-016-2954-9

Li, X., D. Long, Q. Huang, and F. Zhao. 2021. The state and fate of lake ice thickness in the Northern Hemisphere. Sci. Bull. **67**: 537–546. doi:10.1016/j.scib.2021.10.015

Marshall, W., and J. Laybourn-Parry. 2002. The balance between photosynthesis and grazing in Antarctic mixotrophic cryptophytes during summer: *Cryptophytes in Antarctic lakes*. Freshw. Biol. **47**: 2060–2070. doi:10.1046/j.1365-2427.2002.00950.x

Meyer-Jacob, C., N. Michelutti, A. M. Paterson, B. F. Cumming, W. B. Keller, and J. P. Smol. 2019. The browning and re-browning of lakes: Divergent lake-water organic carbon trends linked to acid deposition and climate change. Sci. Rep. **9**: 16676. doi:10.1038/s41598-019-52912-0

NTL-LTER. 2020. North temperate lakes LTER: Chemical limnology of primary study lakes: Nutrients, pH and carbon 1981—Current. Environmental Data Initiative. 10.6073/pasta/8359d27bbd91028f222d923a7936077d

NTL-LTER. 2022. North temperate lakes LTER: Chlorophyll—trout lake area 1981—current ver 30. Environmental Data Initiative. doi:10.6073/pasta/6c8ee65f6876a7274bfe7714ae7c3a70

Obertegger, U., and M. Manca. 2011. Response of rotifer functional groups to changing trophic state and crustacean community. J. Limnol. **70**: 231–238. doi:10.4081/jlimnol.2011.231

Obertegger, U., H. A. Smith, G. Flaim, and R. L. Wallace. 2011. Using the guild ratio to characterize pelagic rotifer communities. Hydrobiologia **662**: 157–162. doi:10.1007/s10750-010-0491-5

Oh, H.-J., H.-G. Jeong, G.-S. Nam, Y. Oda, W. Dai, E.-H. Lee, D. Kong, S.-J. Hwang, and Chang, K.- H. 2017. Comparison of taxon-based and trophi-based response patterns of rotifer community to water quality: Applicability of the rotifer functional group as an indicator of water quality. Anim.

Cells Syst. **21**: 133–140. doi:10.1080/19768354.2017.1292952

Öterler, B. 2017. Winter phytoplankton composition occurring in a temporarily ice-covered lake: A case study. Pol. J. Environ. Stud. **26**: 2677–2688. doi:10.15244/pjoes/74015

Özkundakci, D., A. S. Gsell, T. Hintze, H. Tauscher, and R. Adrian. 2016. Winter severity determines functional trait composition of phytoplankton in seasonally ice-covered lakes. Global Change Biol. **22**: 284–298. doi:10.1111/gcb.13085

Oksanen, J., G. L. Simpson, F. G. Blanchet, R. Kindt, P. Legendre, P. R. Minchin, R.B. O'Hara, P. Solymos, M. Henry H. Stevens, E. Szoecs, H. Wagner, M. Barbour, M. Bedward, B. Bolker, D. Borcard, G. Carvalho, M. Chirico, M. De Caceres, S. Durand, H. B. Antoniazi Evangelista, R. FitzJohn, M. Friendly, B. Furneaux, G. Hannigan, M. O. Hill, L. Lahti, D. McGlinn, M. H. Ouellette, E. R. Cunha, T. Smith, A. Stier, C. J. F. Ter Braak and J. Weedon (2020). vegan: Community ecology package. R package version 2.6-4. Available from https://CRAN.R-project.org/package=vegan

Patriarche, J. D., J. C. Priscu, C. Takacs-Vesbach, L. Winslow, K. F. Myers, H. Buelow, R. M. Morgan-Kiss, and P. T. Doran. 2021. Year-round and long-term phytoplankton dynamics in Lake Bonney, a permanently ice-covered Antarctic Lake. J. Geophys. Res. Biogeosci. **126**: 1–20. doi:10.1029/2020JG005925

Penczykowski, R. M., B. M. Connolly, and B. T. Barton. 2017. Winter is changing: Trophic interactions under altered snow regimes. Food Webs **13**: 80–91. doi:10.1016/j.fooweb.2017.02.006

Perga, M., M. Syarki, J. E. Spangenberg, V. Frossard, E. Lyautey, N. Kalinkina, and D. Bouffard. 2021. Fasting or feeding: A planktonic food web under lake ice. Freshw. Biol. **66**: 570–581. doi:10.1111/fwb.13661

Pernica, P., R. L. North, and H. M. Baulch. 2017. In the cold light of day: The potential importance of under-ice convective mixed layers to primary producers. Inland Waters **7**: 138–150. doi:10.1080/20442041.2017.1296627

Pedersen, T. L. (2022). patchwork: The composer of plots. R package version 1.1.2. Available from https://CRAN.R-project.org/package=patchwork

Phillips, K. A., and M. W. Fawley. 2002. Winter phytoplankton blooms under ice associated with elevated oxygen levels. J. Phycol. **38**: 1068–1073. doi:10.1046/j.1529-8817.2002.01044.x

Powers, S. M., S. G. Labou, H. M. Baulch, R. J. Hunt, N. R. Lottig, S. E. Hampton, and E. H. Stanley. 2017. Ice duration drives winter nitrate accumulation in north temperate lakes. Limnol. Oceanogr. Lett. **2**: 177–186. doi:10.1002/lol2.10048

Rautio, M., H. Mariash, and L. Forsström. 2011. Seasonal shifts between autochthonous and allochthonous carbon contributions to zooplankton diets in a subarctic lake. Limnol. Oceanogr. **56**: 1513–1524. doi:10.4319/lo.2011.56.4.1513

R Core Team (2021). R: A language and environment for statistical computing. R Foundation for Statistical Computing. Available from https://www.R-project.org/

Salmaso, N., and J. Padisák. 2007. Morpho-functional groups and phytoplankton development in two deep lakes (Lake Garda, Italy and Lake Stechlin, Germany). Hydrobiologia **578**: 97–112. doi:10.1007/s10750-006-0437-0

Sanders, R. W., K. G. Porter, and S. J. Bennett. 1990. Heterotrophic, autotrophic, and mixotrophic nanoflagellates: Seasonal abundances and bacterivory in a eutrophic lake. Limnol. Oceanogr. **35**: 1821–1832. doi:10.4319/lo.1990.35.8.1821

Sarma, S. S. S., S. Nandini, and H. J. Dumont. 1997. Feeding preference and population growth of *Asplanchna brightwelli* (Rotifera) offered two non-evasive prey rotifers. Hydrobiologia **361**: 77–88. doi:10.1023/A:1003189312452

Schmitz, O. J., and others. 2014. Animating the carbon cycle. Ecosystems **17**: 344–359. doi:10.1007/s10021-013-9715-7

Schwaderer, A. S., K. Yoshiyama, P. de Tezanos Pinto, N. G. Swenson, C. A. Klausmeier, and E. Litchman. 2011. Eco-evolutionary differences in light utilization traits and distributions of freshwater phytoplankton. Limnol. Oceanogr. **56**: 589–598. doi:10.4319/lo.2011.56.2.0589

Shade, A., and others. 2012. Lake microbial communities are resilient after a whole-ecosystem disturbance. ISME J. **6**: 2153–2167. doi:10.1038/ismej.2012.56

Sharma, S., and others. 2021. Loss of ice cover, shifting phenology, and more extreme events in Northern Hemisphere Lakes. J. Geophys. Res. Biogeo. **126**: 1–12. doi:10.1029/2021JG006348

Shatwell, T., W. Thiery, and G. Kirillin. 2019. Future projections of temperature and mixing regime of European temperate lakes. Hydrol. Earth Syst. Sci. **23**: 1533–1551. doi:10.5194/hess-23-1533-2019

Slatyer, R. A., K. D. L. Umbers, and P. A. Arnold. 2022. Ecological responses to variation in seasonal snow cover. Conserv. Biol. **36**: e13727. doi:10.1111/cobi.13727

Sommer, U., Z. M. Gliwicz, W. Lampert, and A. Duncan. 1986. The PEG-model of seasonal succession of planktonic events in fresh waters. Arch. Hydrobiol. **106**: 433–471.

Sommer, U., and A. Lewandowska. 2011. Climate change and the phytoplankton spring bloom: Warming and overwintering zooplankton have similar effects on phytoplankton: Warming, zooplankton and phytoplankton spring bloom. Global Change Biol. **17**: 154–162. doi:10.1111/j.1365-2486.2010.02182.x

Slowikowski, K. (2021). ggrepel: Automatically Position Non-Overlapping Text Labels with "ggplot2." R package version 0.9.3. Available from https://CRAN.R-project.org/package=ggrepel

Stelzer, C.-P. 1998. Feeding behaviour of the rotifer *Ascomorpha ovalis*: Functional response, handling time and exploitation of individual *Ceratium* cells. J. Plankton Res. **20**: 1131–1144. doi:10.1093/plankt/20.6.1131

Sweeney, K., G. Rollwagen-Bollens, and S. E. Hampton. 2022. Grazing impacts of rotifer zooplankton on a cyanobacteria bloom in a shallow temperate lake (Vancouver Lake, WA, USA). Hydrobiologia **849**: 2683–2703. doi:10.1007/s10750-022-04885-x

Tanabe, Y., S. Kudoh, S. Imura, and M. Fukuchi. 2007. Phytoplankton blooms under dim and cold conditions in freshwater lakes of East Antarctica. Polar Biol. **31**: 199–208. doi:10.1007/s00300-007-0347-2

Vanderploeg, H. A., S. J. Bolsenga, G. L. Fahnenstiel, J. R. Liebig, and W. S. Gardner. 1992. Plankton ecology in an ice-covered bay of Lake Michigan: Utilization of a winter phytoplankton bloom by reproducing copepods. Hydrobiologia **243-244**: 175–183. doi:10.1007/BF00007033

Virro, T., J. Haberman, M. Haldna, and K. Blank. 2009. Diversity and structure of the winter rotifer assemblage in a shallow eutrophic northern temperate Lake Vortsjarv. Aquat. Ecol. **43**: 755–764. doi:10.1007/s10452-009-9276-1

Wang, Q., K. Feng, X. Du, J. Yuan, J. Liu, and Z. Li. 2022. Effects of land use and environmental gradients on the taxonomic and functional diversity of rotifer assemblages in lakes along the Yangtze River, China. Ecol. Indic. **142**: 109199. doi:10.1016/j.ecolind.2022.109199

Weyhenmeyer, G. A., and others. 2022. Towards critical white ice conditions in lakes under global warming. Nat. Commun. **13**: 4974. doi:10.1038/s41467-022-32633-1

Williamson, C. E., E. P. Overholt, R. M. Pilla, T. H. Leach, J. A. Brentrup, L. B. Knoll, E. M. Mette, and R. E. Moeller. 2016. Ecological consequences of long-term browning in lakes. Sci. Rep. **5**: 18666. doi:10.1038/srep18666

Wissel, B., W. J. Boeing, and C. W. Ramcharan. 2003. Effects of water color on predation regimes and zooplankton assemblages in freshwater lakes. Limnol. Oceanogr. **48**: 1965–1976. doi:10.4319/lo.2003.48.5.1965

Wickham, H., and others. 2019. Welcome to the tidyverse. J. Open Sour. Softw. **4**: 1686. doi:10.21105/joss.01686

Wollrab, S., L. Izmest'yeva, S. E. Hampton, E. A. Silow, E. Litchman, and C. A. Klausmeier. 2021. Climate change-driven regime shifts in a planktonic food web. Am. Nat. **197**: 281–295. doi:10.1086/712813

Yang, B., M. G. Wells, J. Li, and J. Young. 2020. Mixing, stratification, and plankton under lake-ice during winter in a large lake: Implications for spring dissolved oxygen levels. Limnol. Oceanogr. **65**: 2713–2729. doi:10.1002/lno.11543

Yoshida, T., and others. 2003. Seasonal dynamics of primary production in the pelagic zone of southern Lake Baikal. Limnology **4**: 53–62. doi:10.1007/s10201-002-0089-3

Acknowledgments

We would like to thank the two reviewers and the associate editor that provided thoughtful feedback that helped us better this manuscript. Thanks to Paul Schramm for plowing so much snow, helping process chlorophyll samples, and offering your wisdom on all field-work logistics. Thanks to the NTL-LTER base crew for helping process our chemical samples. This project was made possible by funding from the US National Science Foundation (DEB-1856224, DEB-2025982), an Anna Grant Birge Award, and a University of Wisconsin-Madison UW-2020 award.

Conflict of Interest

We declare no conflicts of interest.

Submitted 31 August 2022
Revised 01 January 2023
Accepted 05 February 2023

Associate editor: John A. Downing